

# Recombinase-Mediated Cassette Exchange as a Novel Method To Study Somatic Hypermutation in Ramos Cells

Linda B. Baughn,<sup>a\*</sup> Susan L. Kalis,<sup>a</sup> Thomas MacCarthy,<sup>b</sup> Lirong Wei,<sup>a</sup> Manxia Fan,<sup>a</sup> Aviv Bergman,<sup>b</sup> and Matthew D. Scharff<sup>a</sup>

Departments of Cell Biology<sup>a</sup> and Systems and Computational Biology,<sup>b</sup> Albert Einstein College of Medicine, Bronx, New York, USA

\* Present address: Department of Genetics, Cell Biology and Development, University of Minnesota, Minneapolis, Minnesota, USA.

**ABSTRACT** Activation-induced cytidine deaminase (AID) mediates the somatic hypermutation (SHM) of immunoglobulin (Ig) variable (V) regions that is required for the generation of antibody diversity and for the affinity maturation of the antibody response against infectious agents and toxic substances. AID preferentially targets WRC (W = A/T, R = A/G) hot spot motifs, particularly WGCW motifs that create overlapping hot spots on both strands. In order to gain a better understanding of the generation of antibody diversity and to create a platform for the *in vitro* generation of affinity-matured antibodies, we have established a system involving recombinase-mediated cassette exchange (RMCE) to replace the V region and its flanking sequences. This makes it possible to easily manipulate the sequence of the Ig gene within the endogenous heavy chain of the Ramos human Burkitt's lymphoma cell line. Here we show that the newly integrated wild-type (WT) VH regions introduced by RMCE undergo SHM similarly to non-RMCE-modified Ramos cells. Most importantly, we have shown that introducing a cluster of WGCW motifs into the complementary determining region 2 (CDR2) of the human heavy chain V region significantly raised the mutation frequency and number of mutations per sequence compared to WT controls. Thus, we have demonstrated a novel platform in Ramos cells whereby we can easily and quickly manipulate the endogenous human VH region to further explore the regulation and targeting of SHM. This platform will be useful for generating human antibodies with changes in affinity and specificity *in vitro*.

**IMPORTANCE** An effective immune response requires a highly diverse repertoire of affinity-matured antibodies. Activation-induced cytidine deaminase (AID) is required for somatic hypermutation (SHM) of immunoglobulin (Ig) genes. Although a great deal has been learned about the regulation of AID, it remains unclear how it is preferentially targeted to particular motifs, to certain locations within the Ig gene and not to other highly expressed genes in the germinal center B cell. This is an important question because AID is highly mutagenic and is sometimes mistargeted to other highly expressed genes, including proto-oncogenes, leading to B cell lymphomas. Here we describe how we utilize recombinase-mediated cassette exchange (RMCE) to modify the sequence of the endogenous heavy chain locus in the Ramos Burkitt's lymphoma cell line. This platform can be used to explore the regulation and targeting of SHM and to generate human antibodies with changes in affinity and specificity *in vitro*.

Received 13 August 2011 Accepted 21 September 2011 Published 11 October 2011

**Citation** Baughn LB, et al. 2011. Recombinase-mediated cassette exchange as a novel method to study somatic hypermutation in Ramos cells. *mBio* 2(5):e00186-11. doi:10.1128/mBio.00186-11.

**Invited Editor** Myron Goodman, University of Southern California **Editor** Christine Biron, Brown University

**Copyright** © 2011 Baughn et al. This is an open-access article distributed under the terms of the Creative Commons Attribution-Noncommercial-Share Alike 3.0 Unported License, which permits unrestricted noncommercial use, distribution, and reproduction in any medium, provided the original author and source are credited.

Address correspondence to Matthew D. Scharff, matthew.scharff@einstein.yu.edu.

An effective immune response against infectious agents and toxic substances requires the generation of a highly diverse repertoire of antibodies that bind with strong affinity. Initially antibodies are diversified by the combinatorial rearrangement of germ line immunoglobulin (Ig) variable (V), diversity (D), and joining (J) gene segments to create the heavy (H) and light (L) chain V regions. As B cells interact with antigen and differentiate into antibody-secreting cells, these rearranged V regions undergo a further diversification process called somatic hypermutation (SHM) to produce higher-affinity antibodies that may also have changes in fine specificity (1). While much has been learned about the generation of a diverse and high-affinity repertoire, many details of how this process is regulated and targeted to antibody genes are still poorly understood (2). To achieve a better understanding

of this highly mutagenic process, it would be useful to have new platforms to study the generation of antibody diversity and the affinity maturation of the immune response. Such platforms would also be useful in generating better monoclonal antibodies for solving many scientific questions and to diagnose and treat disease.

Activation-induced cytidine deaminase (AID) is required for and initiates SHM (3, 4) by deaminating dC residues of single-stranded DNA (ssDNA) within transcription bubbles, creating a guanine-uracil (G-U) mismatch. These mismatched bases are either processed during replication, resulting in C-to-T transitions; removed by uracil-DNA glycosylase (UNG) during short-patch base excision repair (BER); or excised by mismatch repair (MMR), where the excised DNA strand is resynthesized in an

error-prone manner, creating additional mutations (2, 5, 6). AID preferentially targets cytosines for deamination in WRC hot spot (HS) motifs (7–10), but very little is known about exactly how this targeting is achieved or why the V regions and not the C region and most other non-Ig genes are not usually targeted (11–13). One way to examine the mechanisms and identify the factors responsible for the preferential targeting of AID would be to change the sequences in the Ig V region and its immediate flanking sequences and regulatory regions. This is preferably done within the endogenous locus, since all of the *cis*-acting sequences required for this process have yet to be determined. Antibody-forming B cell lines in tissue culture allow the examination of multiple different engineered versions of parts of the Ig gene, but such experiments require the repeated replacement of the wild-type (WT) Ig gene by the modified H or L chain genes (14). Currently, this is most often done using the DT40 cell line, which has a high frequency of homologous recombination (15, 16). However, DT40 is a chicken B cell line where the somatic V region mutation process coexists with gene conversion. Even though the competition between SHM and gene conversion can be overcome using genetically modified versions of DT40 (17–19), these cells do not express the second phase of SHM involving BER and MMR that is responsible for the acquisition of large numbers of mutations in A-T residues, and in this and probably other ways, the mutational process in DT40 cells differs from that which occurs in mouse and human B cells (20, 21).

The frequency of homologous recombination in the IgH locus in centroblast-like human Epstein-Barr virus-negative (EBV<sup>-</sup>) Burkitt's lymphoma cell lines is quite high (22), but these cell lines would be even more useful if the replacements could be restricted to the rearranged IgH chain locus in a way that favored the replacement of only the endogenous gene and the insertion of the transfected gene in the correct orientation. Here we describe the use of the recombinase-mediated cassette exchange (RMCE) strategy (23–26) as a technique that can be used to easily manipulate the sequence of the Ig gene within the endogenous locus of the Ramos human Burkitt's lymphoma B cell line. Ramos cells are an excellent cell line for this system because they constitutively express AID and undergo SHM in tissue culture (27–30), are easily transfectable, have only one rearranged IgH chain V region, express large amounts of surface IgM $\lambda$ , and secrete only small amounts of antibody. It has already been shown that these properties allow the use of fluorescence-activated cell sorting of Ramos cells to sequentially select for rare cells, making variants of the endogenous Ramos antibody that have a higher affinity and changes in specificity and thus can mimic the affinity maturation of normal human antibodies (31). This suggests that if the Ramos IgH V regions could be readily replaced by other V regions, this platform could be used to affinity mature and change the fine specificity of many different monoclonal antibodies.

Here we describe how to use RMCE to replace the endogenous IgH V region, and we show that the newly inserted wild-type V region undergoes SHM at approximately the same rate and with the same characteristics as that in the original wild-type Ramos cells. By engineering a replacement construct with multiple cloning sites, we can insert any V region in place of the endogenous IgH V region and easily manipulate the sequence of the V region as well as surrounding *cis* regulatory sequences at the endogenous locus. We also demonstrate that we can increase the relatively low spontaneous rate of mutation seen in all cultured cells (32) by

introducing a cluster of hot spots into the highly mutable complementary determining region 2 (CDR2) of the V region without changing the distribution or characteristics of the mutational process. This indicates that the Ramos cells provide a useful platform for examining the role of the V region sequence environment and of *cis*-acting elements and for affinity maturing of human antibodies to any antigen.

## RESULTS

**Replacing the endogenous IgH VDJ and flanking regions of Ramos cells with Hyg-TK.** To establish RMCE (23) in Ramos cells, we created a number of constructs that could be homologously recombined into the endogenous H chain locus. First, a targeting construct (Fig. 1A) was generated that contained 2.2 kb of sequence 5' to the promoter of the endogenous rearranged VH 4–34 gene (5' homologous arm), a lox site (lox), the hygromycin and thymidine kinase resistance genes (Hyg-TK) driven by a cytomegalovirus (CMV) promoter, a second lox (lox) site that differs from the first lox site to facilitate directional integration, and 5.8 kb of sequences 3' to the  $\mu$  switch region that include all of the  $\mu$  constant region and the membrane and secretory exons (3' homologous arm). When the targeting construct was transfected into surface IgM-positive Ramos cells, ~2% (5/235) of the transfected cells were hygromycin resistant and surface IgM negative. Since they had lost their surface IgM, it was likely that they had undergone homologous replacement of the H chain V, E $\mu$ , or S $\mu$  (Fig. 1A). To confirm this, all five of the independently transfected IgM<sup>-</sup> hygromycin-resistant clones were analyzed by Southern analysis and compared to the original unmodified Ramos clone (labeled "C" for control) (Fig. 1B). This revealed that the productive endogenous IgH gene had been disrupted while the other Ramos endogenous IgM gene that had previously undergone translocation with Myc was still present. Using primer P1, located outside the targeting construct, and primer P2, located within the targeting construct (Fig. 1A), PCR analysis of genomic DNA from each of the 5 independently transfected clones further confirmed that the Hyg-TK gene was present and in the correct orientation (Fig. 1C). The presence of the Hyg-TK gene and the loss of the productive  $\mu$  gene established that the Hyg-TK gene had homologously recombined into the endogenous productive H chain locus and that the targeting construct was in the correct orientation.

**Cre-mediated replacement of the Hyg-TK with the Ramos V region.** Next, we transfected a wild-type replacement construct containing lox (2L)-VDJ-E $\mu$ -S $\mu$ -lox (L3) (WT A) (Fig. 2) into the Hyg-TK-expressing cells (Hyg-TK) along with a Cre expression plasmid and allowed it to recombine at the lox sites (primary replacement of Hyg-TK). The TK gene was present so that we could have counterselected with ganciclovir for clones in which the Hyg-TK was replaced (23). However, we found that the Ramos cells were very sensitive to ganciclovir, and it was difficult to find a dose that did not kill some of the TK-negative cells. Since in this case the clones that had successfully integrated the replacement vector expressed surface IgM, recovering IgM<sup>+</sup> cells by fluorescence-activated cell sorting provided an easy and reliable counterselection in which virtually all of the counterselected cells expressed the replacement vector. We therefore elected to isolate integrated clones by sorting for IgM and cloning IgM<sup>+</sup> cells in soft agar. The isolation and subsequent characterization (see below) of these IgM<sup>+</sup> cells demonstrated that the endogenous H chain gene could be easily restored in Ramos cells.

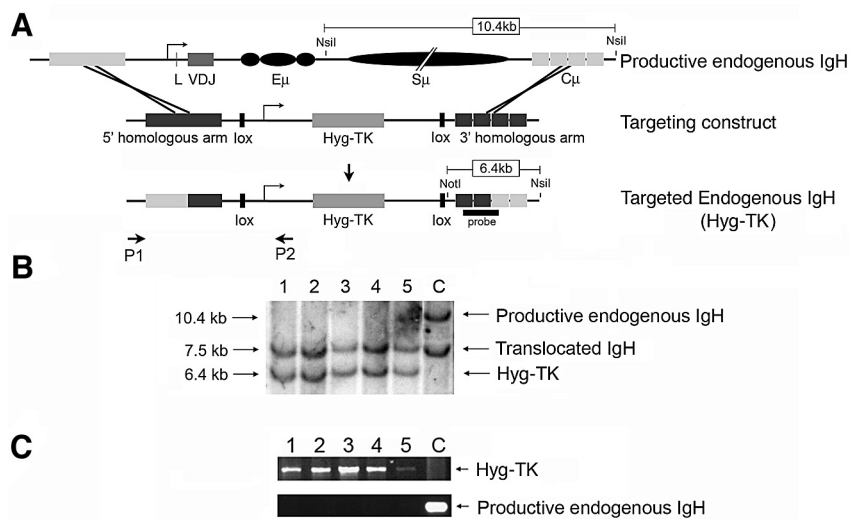


**FIG 1** Schematic of the recombinase-mediated cassette exchange strategy. (A) Homologous recombination to create the Hyg-TK Ramos cell line. A schematic of the productive endogenous IgH allele includes the leader exon (L), the variable region (VDJ), E $\mu$ , S $\mu$ , and C $\mu$ . The 5' and 3' homologous arms, the lox sites, and the location of the Hyg-TK gene are depicted in the targeting construct. (B) Southern blot of 5 independently isolated Hyg-TK RMCE clones and a control (lane C) IgM<sup>+</sup> wild-type non-RMCE Ramos clone. DNA was digested with NotI and NsiI, shown in panel A, and hybridized with a C $\mu$  probe depicted by the black diagonal line in panel A. (C) PCR analysis using genomic DNA of the same clones described in panel B using primers P1 and P2 shown in panel A.

In order to determine whether these newly created WT A RMCE clones could undergo a second round of replacement, we transfected still another replacement construct that contains a C-to-G mutation at position 237 located within framework 2, creating a nonsense mutation (WT B) (Fig. 2 and 3A) into the WT A clones along with a Cre expression plasmid and allowed it to recombine at the lox sites. In this case, the successfully integrated clones did not express surface IgM due to their nonsense codon, so we recovered IgM<sup>-</sup> cells by fluorescence-activated cell sorting. The successful replacement of the WT A insert by WT B demonstrated that a secondary replacement of the endogenous H chain gene could be achieved in Ramos cells that had already undergone one replacement. Independently derived WT A and WT B clones were each subcloned, and the WT A and B subclones were found to express similar levels of AID transcripts (Fig. 3B).

**RMCE clones undergo SHM with WT frequency and characteristics.** To confirm that cassette exchange would allow a replaced gene to function like the WT gene, we grew constitutively mutating Ramos clones with the newly inserted V regions for 1.5 months to accumulate a sufficient number of mutations and

sequenced random V regions as we have done in the past (30, 33). Ramos cells have only one rearranged V region, allowing us to amplify only the V region that was successfully integrated in the correct location using primers that anneal upstream of the first lox site and within JH6 (Fig. 3A, primers P3 and P4). Since it is possible that some mutations could have arisen during the cassette exchange (34), cells were collected immediately following subcloning and their V regions were sequenced and found to not contain new mutations. Additionally, only unique mutations were scored in order to eliminate the possibility that “founder mutations” that arose before the start of the experiment would bias the results, although this results in the loss of some mutations which occur recurrently in hot spots and thus leads to an underestimate of the frequency of mutation. Sequence analysis of random V regions (between primers P3 and P4 shown in Fig. 3A; also Table 1) from the progeny of Ramos subclones WT A and WT B undergoing constitutive SHM revealed no significant differences ( $P = 0.6109$ ,  $\chi^2$  test) in the frequency of unique mutations between the two sequentially replaced V regions (Fig. 3C; Table 1). This showed that, as reported in other systems (35), the small amount

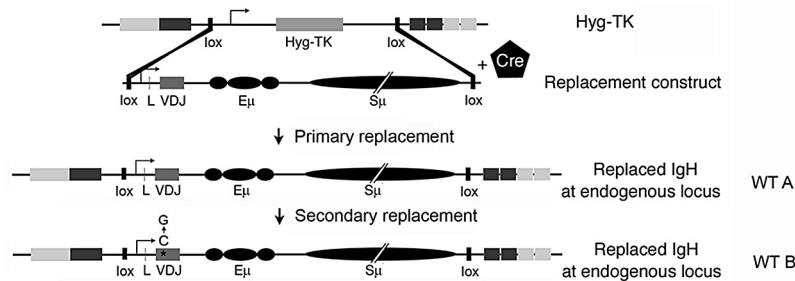


**FIG 2** Schematic of the Cre-mediated recombination to create the replaced IgH at the endogenous locus. The pentagon represents the addition of Cre, and the arrows demonstrate the transfection of WT A to create the primary replacement and the transfection of WT B to create the secondary replacement. The asterisk indicates the C-to-G mutation within VDJ of WT B.

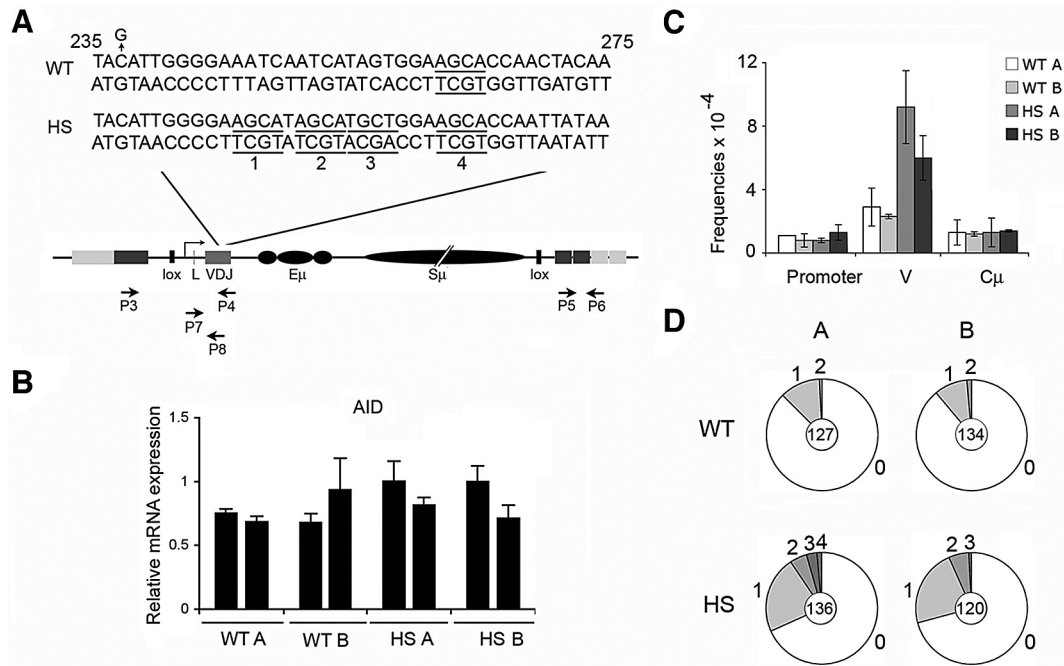


**FIG 3** Insertion of a cluster of hot spots into the endogenous heavy chain gene of Ramos cells increases V region mutation. (A) Schematic of the replaced IgH locus with primer pairs used for amplification and sequencing indicated by arrows (P3 to P8). (B) Relative AID transcript levels in the various subclones shown in the bar graph with standard deviations. (C) A bar graph showing the frequencies of mutations depicted in Table 1 from the promoter, V, and constant regions. Error bars represent the standard deviations between 2 clones. (D) Pie charts representing the number of mutations per sequence; the number of sequences analyzed is depicted in the center of each circle.

of nonsense-mediated decay induced by a nonsense mutation in WT B that was close to the promoter did not affect the rate of V region mutation (Fig. 3C). The newly inserted WT A and WT B V regions underwent a similar frequency of mutation as did the original parental wild-type Ramos cells (29, 30, 33) that were used to create the RMCE clones.

To determine whether the RMCE process mistargets AID to the regions of the Ig gene flanking V which normally do not undergo SHM (11, 12, 36), we have also sequenced the promoter region from the 2L site to the leader exon (between primers P3 and P8) as well as the functional Cμ (37) from the CH1 exon to the CH2 intron (Fig. 3A, between primers P5 and P6). Although we detected a few mutations ( $0.8 \times 10^{-4}$  to  $1.3 \times 10^{-4}$  mutations/

bp) in the promoter and constant regions (Fig. 3C; Table 1), the mutation frequency was statistically significantly lower than the frequency of V region mutations (V versus promoter,  $P = 0.002$ ; V versus Cμ,  $P = 0.03$ ) and these mutations were not in AID hot spots, suggesting that these low-frequency mutations likely arose from PCR error (33). This is in contrast to the V region, where 39% of the mutations in WT RMCE clones were in WRCY/RGYW AID hot spot motifs, similar to the original parental wild-type Ramos cells (29).

Furthermore, Ramos RMCE clones showed characteristics of the mutations in the V regions similar to those of the parental wild-type Ramos cells in that ~85 to 90% of the mutations were in G-C residues (see Table S1 in the supplemental material). The

**TABLE 1** Mutations from WT and HS cell lines<sup>a</sup>

Region	Clone	No. of unique mutations	Total bp sequenced	Frequency ( $10^{-4}$ )
Promoter	WT A	7	63,392	1.1
	WT B	6	75,278	0.8
	HS A	4	63,958	0.8
	HS B	6	45,846	1.3
VH	WT A	17	58,166	2.9
	WT B	14	61,372	2.3
	HS A	57	62,288	9.2
	HS B	33	54,960	6.0
Cμ	WT A	6	46,848	1.3
	WT B	7	58,560	1.2
	HS A	7	53,436	1.3
	HS B	6	43,920	1.4

<sup>a</sup> The promoter region was amplified using primers P3 and P4 and sequenced using primer P8. This region corresponds to a 566-bp region from the 2L lox site to the leader exon. The V region was amplified using primers P3 and P4 and sequenced using primer P7. This region corresponds to a 458-bp region from the leader intron to the end of JH6. The functional Cμ was amplified using primers P5 and P6 and sequenced using primer P5. This region corresponds to a 732-bp region from the CH1 exon to the CH2 intron.

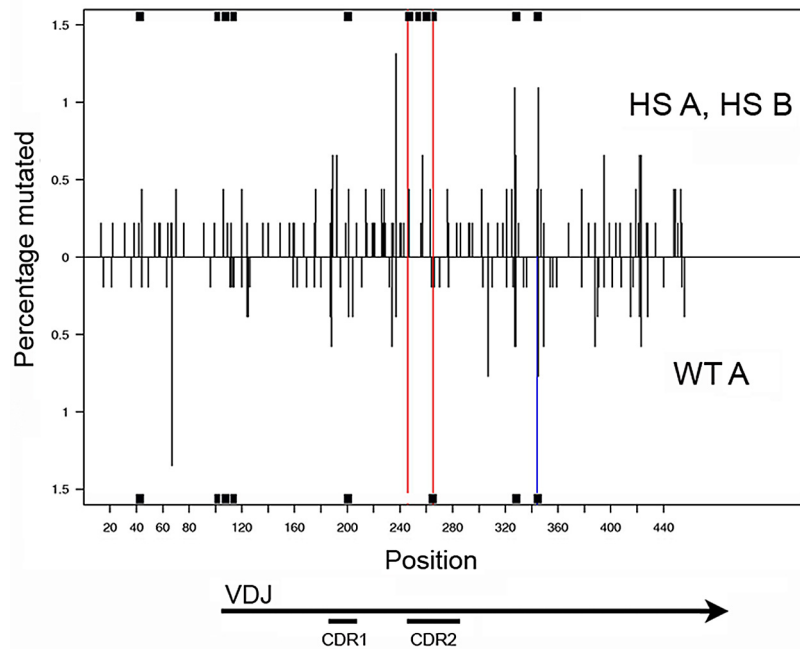


**FIG 4** Distribution of mutations in WT and HS clones. Distribution of total mutations in the 458-bp VDJ region of HS A and B clones compared to WT A. The red line indicates the boundary of the hot spot cluster. Some sequences were dominated by a single highly mutated site which was removed from the analysis and replaced by the blue line in order to display the results on the same  $y$  axis scale. The black boxes represent the WGCW motifs. In order to increase the number of mutations examined, additional sequences from WT A and HS A and B subclones not shown in the previous figures and Table 1 were added to this figure.

mutations also occurred in locations similar to those of non-RMCE-derived Ramos mutations, since the moving average of mutation frequencies (see Materials and Methods) has a correlation of 0.79 ( $P < 2 \times 10^{-16}$ ).

**Insertion of a cluster of hot spots into the endogenous heavy chain gene of Ramos cells increases the frequency of mutation throughout the V region.** As in other cultured mouse and human B cell lines (32), the overall frequency of mutation in the V regions was  $2 \times 10^{-4}$  to  $4 \times 10^{-4}$ , which is only 2- to 3-fold greater than the PCR error (Table 1) and  $\sim 10$ -fold lower than the frequencies of mutation that are seen *in vivo* in germinal center B cells (2, 38). As a consequence, only a small percentage of randomly sequenced Ramos V regions contain new unique mutations (Fig. 3D), and in the V regions that have undergone SHM, the number of new mutations that accumulate even after 1 to 3 months, while orders of magnitude higher than that in non-Ig genes, is small compared to the PCR error (Fig. 3; Table 1). We therefore explored ways to increase the frequency of mutation in the Ramos cell line so as to make it more useful as a tool to explore the effect of changes in the local sequence environment and of *cis*-acting sequences on the distribution and characteristics of mutations in the V region and to generate better antibodies more quickly.

An extension of the WRC motif, the WGCW motif, particularly the AGCT variant of that motif, has been demonstrated to be highly susceptible to AID mutation (9, 10, 39–43). The WGCW motif represents an overlapping hot spot (a hot spot on both the top and bottom strands) within which the adjacent C's on opposite strands could be targeted for mutation. This motif is enriched in mammalian switch regions (44) and has been identified as a site of focusing of mutations *in vivo* in the absence of repair (41–43). With the thought that a cluster of hot spots could act as an entry or

activation site for AID, we engineered a cluster of 4 WGCW hot spots within the CDR2 of the Ramos IgH V gene to create 8 total hot spots within a 20-bp stretch on both the upper and lower strands (Fig. 3A) without changing the amino acid sequence of the VH region. This V region with its cluster of HSs was introduced into two different Ramos subclones by RMCE (HS A and HS B in Fig. 3), and the frequency of mutation was determined by sequencing (Fig. 3; Table 1). These HS cluster clones had a statistically significant  $\sim 2$ - to 4-fold increase in the frequency of unique mutations compared to the WT RMCE controls (Fig. 3C; Table 1) (WT A/B versus HS A,  $P < 0.0001$ ; WT A/B versus HS B,  $P = 0.0009$ ; HS A versus HS B,  $P < 0.0664$ ). This was associated with a larger number of mutated V regions, and there were more V regions with greater than 1 mutation per V (Fig. 3D) (WT A/B versus HS A,  $P = 0.0002$ ; WT A/B versus HS B,  $P = 0.0079$ ). While the overall frequency of unique mutations in the V regions with the HS cluster was increased, the characteristics of the mutations in the V regions with the HS cluster resemble the WT in that  $\sim 85$  to 90% of the mutations were in G-C residues (see Table S1 in the supplemental material). While it was possible that the AID-induced mutations could have been concentrated in and around the HS cluster, this did not occur, and the mutations were distributed throughout the V region in a pattern that was similar to that of the WT RMCE clones (Fig. 4; see also Fig. S1). We repeated the moving average analysis (see Materials and Methods) comparing the distribution of mutations in the HS cluster and WT V regions and again found a highly significant positive correlation ( $r = 0.52$ ,  $P < 2 \times 10^{-16}$ ). Thus, we have demonstrated that the insertion of a V region by RMCE in Ramos cells containing a cluster of overlapping hot spots increases the frequency of mutation without changing their characteristics or distribution.

## DISCUSSION

When AID and Ig genes are introduced into non-B cells and B cell lines, the transfected Ig genes will undergo AID-induced mutations, especially if they are surrounded by Ig regulatory elements and if AID is overexpressed (29, 33). In addition, transfected non-Ig genes, including AID itself, can undergo AID-induced mutations in B and non-B cells (33). Perhaps one of the most useful examples of this was the generation of red fluorescent protein (RFP) molecules with new and useful properties when RFP was introduced into Ramos cells that were constitutively expressing AID (45). These transfected cell systems have made it possible to study some aspects of the regulation of AID targeting and to change the properties of Ig and non-Ig proteins. Studies with mutant mice and biochemical analysis have revealed some of the associated proteins that contribute to higher mutation rates in Ig genes (46–50). Although some *cis*-acting sequences have been shown to have a role in targeting AID to antibody V regions (15, 51) and structure-function studies with AID have revealed the parts of the enzyme that are responsible for recognizing hot spot motifs (52–55), much remains to be learned about these aspects of the mutational process.

To facilitate such studies, we have modified the Ramos human Burkitt's lymphoma cell line so that the structure of the IgH V regions and its immediate flanking sequences can be readily and repeatedly modified using RMCE. In this study, we have shown that once the endogenous VH and its flanking regulatory regions are replaced by the RMCE targeting lox-Hyg-TK-lox gene, modified VH genes can be readily inserted in one copy in the proper orientation into the IgH locus. Ectopic insertions were not detected. In addition, we found that the replaced wild-type VH regions mutated at the same frequencies and with the same characteristics and distribution as did the endogenous Ramos VH regions. In addition to the various modifications of the endogenous Ramos 4–34 VH regions described here, two other human V regions have been introduced by RMCE and found to mutate with frequencies similar to those of the WT 4–34 V region. In order to use this system to affinity mature unrelated human antibodies, it will also be necessary to replace the L chain. While this could be done by establishing a separate RMCE system with different drug markers for the light chain, we have found that a simpler way to do this is to identify subclones of Ramos cells that have the IgH RMCE vector and have lost the ability to make the endogenous L chains. Transfected L chains in ectopic locations do undergo AID-induced mutations, thus allowing the mutation of both the H and L chains if that is required for affinity maturation (data not shown).

A significant problem with using the Ramos system and other cultured B cell systems either to examine the mechanisms of SHM or to make better antibodies or other proteins is that the frequency of AID-induced mutations, while still high compared to the mutation rate throughout the genome, is still ~10-fold lower than that which is observed *in vivo* and only a fewfold higher than the PCR error rate. While this can be overcome to some degree by overexpressing AID, this also causes targeting of the C region and other highly expressed genes such as AID itself (33, 36), making it difficult to study the preferential targeting of AID to antibody V regions. Mutant AID molecules with increased activity increase the mutation rate but also tend to decrease the specific targeting

and the viability of the host cell, presumably due to an increase in AID mutations in critical non-Ig genes (55).

Here we have shown that we can avoid these problems by increasing the frequency of AID-induced mutations in the V region by introducing a cluster of WGCW AID hot spots that lead to overlapping hot spots in the CDR2 of the VH region. This increased the mutation rate 2- to 4-fold so that it begins to approach the *in vivo* frequency of mutation without significantly changing the overall targeting, characteristics, and distribution of mutations within the V region. We confirmed that the increase in mutation was restricted to the VH region that contained the cluster of hot spots by sequencing the endogenous L chain genes in Ramos cells (37) and showing that the frequencies of mutation in the L chains were similar in the WT and HS A and B clones (data not shown). The WGCW motif has been shown to be more highly targeted for mutation *in vivo* (9, 10, 39–43, 56). Because of the high frequency of mutations at such sites within the mouse JH4 intron and S $\mu$  region in the absence of repair (41–43, 57, 58) and in human V regions (10, 59), it has been suggested that it could be a potential site for the entry of AID (40, 42). Since AID is a very inefficient enzyme (60, 61), it is possible that AID accesses the V region elsewhere but is preferentially activated at this motif to initiate the process of mutation. Since AID can form multimeric complexes (62–64), it is also possible that it could preferentially associate with both strands of DNA where there are overlapping hot spots and promote multiple deamination reactions (40, 64). Whatever the explanation, it is surprising that there was not a local increase in mutations in and around the hot spot cluster. Of 11 different subclones expressing the cluster of hot spots, only one revealed an increase of mutations in the region of the cluster (data not shown), and further experiments will be required to determine the true frequency of such clones and the mechanism responsible for the increased focusing of mutation with the hope that such studies will reveal new information on the targeting and activation of AID *in vivo*. While this work was in progress, RMCE was also used in mouse CH12 cells to study detailed sequence requirements for targeting AID to mouse Ig switch regions to mediate class switch recombination (26). These authors concluded that it was the overlapping nature of the WGCW motif, rather than the palindromic characteristics of some representatives of the motif, that increased the likelihood of mutations and subsequent double-stranded DNA breaks in switch regions.

Here we present a novel platform for the modification of the immunoglobulin V region using RMCE in Ramos cells. We have shown here that inserting a cluster of overlapping hot spots in the H chain V region increases the rate of mutation without affecting the characteristics or distribution of those mutations, illustrating how this system will be useful in exploring the regulation and restriction of V region mutations. Since we can also insert new L chains and the Ramos cells have been shown to switch at a low frequency from IgM to IgG expression (65), this system will be useful for the affinity maturation of human monoclonal antibodies.

## MATERIALS AND METHODS

**Cell lines and culture conditions.** The Ramos Burkitt's lymphoma cell line was obtained from Hilda Ye (Albert Einstein College of Medicine, Bronx, NY) and grown in Iscove's modified Dulbecco's medium (IMDM; BioWhittaker, Walkersville, MD) supplemented with 10% fetal bovine serum (Atlanta Biologicals, Lawrenceville, GA) and 100 U/ml penicillin-

streptomycin (Mediatech, Herndon, VA). Soft agar cloning was performed as previously described (30). An IgM<sup>+</sup> subclone of Ramos 6 (30), Ramos 6.25 subclone 8 (6.25), was used as the parental clone for the RMCE system.

**RMCE plasmids.** Details of the construction of the targeting and replacement constructs are located in the supplemental material (see Text S1). Briefly, for the targeting construct, the 5' and 3' homologous arms were constructed by PCR amplification from Ramos clone 6 genomic DNA and the lox and Hyg-TK segments were cloned from the pCR4-TOPO-2L-Hyg-TK-L3 vector (Eric Bouhassira, Albert Einstein College of Medicine, Bronx, NY). Hygromycin-resistant IgM<sup>-</sup> LC<sup>+</sup> Ramos cells transfected with the targeting construct were screened for integration of the targeting construct by PCR using the following primers: P1, 5' CTATGTGGCGAAAGGCAATCTATC 3', which binds upstream of the 5' arm, and P2, 5' GAACTCCATATGGGCTATGAAC 3', which binds within the CMV promoter of the Hyg-TK gene. For the replacement constructs, the pUC VDJ1 E $\mu$ S $\mu$  (WT A) replacement was created from a series of intermediate plasmids detailed in the supplemental materials (see Text S1). The pUC VDJ4-1 E $\mu$ S $\mu$  (WT B) and pUC VDJ hot spot E $\mu$ S $\mu$  (HS) plasmids were created by site-directed mutagenesis by PCR amplification of pUC VDJ1 E $\mu$ S $\mu$  (WT A) as described in the supplemental material (see Text S1).

**Transfection conditions.** Ramos cells were electroporated with either 2  $\mu$ g of the "targeting construct" or 12.5  $\mu$ g of each "replacement construct" along with 3.2  $\mu$ g of Cre using the Nucleofector II (Lonza, Amasa, Cologne, Germany) and Nucleofection (Lonza) kits. pBS 185 CMV-Cre was a gift from Eric Bouhassira (Albert Einstein College of Medicine, Bronx, NY) and was originally obtained from Clontech (Palo Alto, CA). Ramos RMCE clones were selected using 0.6 mg/ml of hygromycin (Calbiochem).

**Fluorescence analysis and sorting.** Ramos cells were stained with goat anti-human IgM-fluorescein isothiocyanate (FITC) (Southern Biotechnology Associates, Birmingham, AL) and analyzed using the FACScan (Becton Dickinson, Franklin Lakes, NJ) cell sorter. For fluorescence-activated cell sorting experiments, at least  $2 \times 10^7$  cells were used, stained as described above, and sorted using a FACSAria (Becton Dickinson) cell sorter.

**Southern blotting.** Genomic DNA from hygromycin-resistant IgM<sup>-</sup> LC<sup>+</sup> Ramos clones (Hyg-TK) was digested with NotI and NsiI, and the DNA fragments were separated on a 0.7% agarose gel, transferred to a Hybond N<sup>+</sup> nylon membrane (GE Healthcare, Amersham Biosciences, Piscataway, NJ) in  $20 \times$  SSC (3 M NaCl plus 300 mM sodium citrate), and UV cross-linked to the membrane. A C $\mu$  probe containing the majority of exons 1 to 3 was generated by digesting the 3' homologous arm DNA with SbfI and HincII, labeled with [ $\gamma$ -<sup>32</sup>P]CTP, hybridized to the blot at 65°C for 2 h, and visualized by autoradiography. Clones containing the targeting vector correctly integrated at the functional C $\mu$  allele produced a ~6.4-kb band as well as a ~7.5-kb band that represented the nonfunctional C $\mu$  allele. Parental clones RMCE 1 and RMCE 3 (Fig. 1B and C) were thus identified and used in this study. No significant difference in mutation frequency was detected when either the RMCE 1 or the RMCE 3 clone was used.

**PCR amplification, cloning, and sequencing.** Genomic DNA was prepared as reported previously (30). The V and C $\mu$  region from Ramos clones were amplified using *Pfu* Turbo Cx Hotstart polymerase from genomic DNA by using 30 cycles of 95°C for 30 s, 60°C for V region or 66°C for C $\mu$  for 30 s, and 72°C for 1 min. Primers for the V region were P3, 5' TGTCTTCAGATCAGCAGCCTAAAG 3' (5' primer), and P4, 5' CAT TCTTACCTGAGGAGACGGTG 3' (3' primer), and for the C $\mu$  region were P5, 5' GCATCCGCCCAACCCCTTTTC 3' (5' primer), and P6, 5' G CGAATGCCAGACCCGAGTG 3' (3' primer). PCR products were modified by A-tailing using *Taq* polymerase and cloned using the pGEM-T vector system. Miniprepations were prepared using the Montage Plasmid Miniprep<sub>HTS</sub> 96 kit (Millipore, Billerica, MA) and sequenced using the ABI 3730 DNA analyzer (Applied Biosystems, Carlsbad, CA). Primers

used for sequencing were the following: V region, P7, 5' GCACAAGAAC ATGAAACACC 3'; IgH promoter region, P8, 5' GGACCCCTGTGAAC AGAAAA 3'; C $\mu$ , P5, as described above. The functional C $\mu$  allele was distinguished from the nonfunctional allele as described previously (37). DNA was analyzed using SeqMan (DNASTar, Madison, WI), and statistical analysis was performed using a chi-square test.

**Extraction of RNA and quantitative real-time RT-PCR.** RNA was extracted as reported previously (30). Five micrograms of RNA was reverse transcribed using the Superscript III first-strand synthesis system (Invitrogen). Quantitative real-time PCR of cDNA was performed in triplicate using the DNA Engine Opticon 2 cycler (MJ Research, Waltham, MA) and QuantiTect SYBR Green (Qiagen) by using 40 cycles of 94°C for 15 s, 60°C for 30 s, and 72°C for 30 s. The following primers were used: IgM, 5' GACAGTCCAAGAAACAGC 3' (5' primer) and 5' GCCCTAG TAATAACTCTCGC 3' (3' primer); AID, 5' CTTCGCAATAAGAACGG CTG 3' (5' primer) and 5' GAGGTGAACCAGGTGACGC 3' (3' primer); glyceraldehyde-3-phosphate dehydrogenase (GAPDH), 5' CTGCGACC GCCCCCGAACCG 3' (5' primer) and 5' TACCCTGCCCCCATACGAC TGCAAAGACC 3' (3' primer). Data were analyzed using the Opticon Monitor 3 program (MJ Research), and relative fold changes in cDNA levels were calculated using the threshold cycle ( $2^{-\Delta\Delta C_T}$ ) method with the GAPDH reference gene as normalization (66).

**Moving average analysis.** Because the mutation frequency in Ramos cells is relatively low, a direct site-by-site comparison of mutation frequencies is inappropriate. We therefore compared the overall patterns of unique mutation frequencies using a moving average, i.e., the mean mutation frequency within a sliding window of length 100 along the length of the sequence. In each case, we also tested with shorter window lengths of 80 and 60 with similar results. We then calculated the correlation between the two moving averages. When comparing data sets with nonidentical germ line sequences, we excluded any sites that were not shared between the two germ line sequences.

## ACKNOWLEDGMENTS

This work was supported by the Albert Einstein College of Medicine Cancer Center Flow Cytometry and DNA Sequencing Cores (P30CA013330) and by grants to M.D.S. (RO1CA72649, RO1CA102705, and U54AI157158) and by the Harry Eagle Chair provided by the National Women's Division of the Albert Einstein College of Medicine. L.B.B. and S.L.K. were supported by 5T32CA91773, and L.B.B. was supported by a grant from the Leukemia and Lymphoma Society. T.M. and A.B. are supported by NIH grants 1-R01-AG028872 and 1-P01-AG027734.

We thank members of the Scharff and B. Birshstein laboratories, M. Sadofsky, and H. Ye for helpful discussions. We thank Eric Bouhassira for RMCE reagents and advice, and we thank Uwe Werling for cloning advice.

## SUPPLEMENTAL MATERIAL

Supplemental material for this article may be found at <http://mbio.asm.org/lookup/suppl/doi:10.1128/mBio.00186-11/-DCSupplemental>.

Figure S1, PDF file, 1.4 MB.

Text S1, DOC file, 0.1 MB.

Table S1, PDF file, 0.1 MB.

## REFERENCES

1. Rajewsky K, Förster I, Cumano A. 1987. Evolutionary and somatic selection of the antibody repertoire in the mouse. *Science* 238:1088–1094.
2. Peled JU, et al. 2008. The biochemistry of somatic hypermutation. *Annu. Rev. Immunol.* 26:481–511.
3. Muramatsu M, et al. 2000. Class switch recombination and hypermutation require activation-induced cytidine deaminase (AID), a potential RNA editing enzyme. *Cell* 102:553–563.
4. Revy P, et al. 2000. Activation-induced cytidine deaminase (AID) deficiency causes the autosomal recessive form of the Hyper-IgM syndrome (HIGM2). *Cell* 102:565–575.
5. Maul RW, Gearhart PJ. 2010. AID and somatic hypermutation. *Adv. Immunol.* 105:159–191.

6. Stavnezer J. 2011. Complex regulation and function of activation-induced cytidine deaminase. *Trends Immunol.* 32:194–201.
7. Jolly CJ, et al. 1996. The targeting of somatic hypermutation. *Semin. Immunol.* 8:159–168.
8. Pham P, Bransteitter R, Petruska J, Goodman MF. 2003. Processive AID-catalyzed cytosine deamination on single-stranded DNA simulates somatic hypermutation. *Nature* 424:103–107.
9. Rogozin IB, Diaz M. 2004. Cutting edge: DGYW/WRCH is a better predictor of mutability at G:C bases in Ig hypermutation than the widely accepted RGYW/WRCY motif and probably reflects a two-step activation-induced cytidine deaminase-triggered process. *J. Immunol.* 172:3382–3384.
10. Ohm-Laursen L, Barington T. 2007. Analysis of 6912 unselected somatic hypermutations in human VDJ rearrangements reveals lack of strand specificity and correlation between phase II substitution rates and distance to the nearest 3' activation-induced cytidine deaminase target. *J. Immunol.* 178:4322–4334.
11. Longerich S, Tanaka A, Bozek G, Nicolae D, Storb U. 2005. The very 5' end and the constant region of Ig genes are spared from somatic mutation because AID does not access these regions. *J. Exp. Med.* 202:1443–1454.
12. Rada C, Milstein C. 2001. The intrinsic hypermutability of antibody heavy and light chain genes decays exponentially. *EMBO J.* 20:4570–4576.
13. Liu M, et al. 2008. Two levels of protection for the B cell genome during somatic hypermutation. *Nature* 451:841–845.
14. Batrak V, Blagodatski A, Buerstedde JM. 2011. Understanding the immunoglobulin locus specificity of hypermutation. *Methods Mol. Biol.* 745:311–326.
15. Tanaka A, Shen HM, Ratnam S, Kodgire P, Storb U. 2010. Attracting AID to targets of somatic hypermutation. *J. Exp. Med.* 207:405–415.
16. Bachl J, Caldwell RB, Buerstedde JM. 2007. Biotechnology and the chicken B cell line DT40. *Cytogenet. Genome Res.* 117:189–194.
17. Sale JE, Calandrini DM, Takata M, Takeda S, Neuberger MS. 2001. Ablation of XRCC2/3 transforms immunoglobulin V gene conversion into somatic hypermutation. *Nature* 412:921–926.
18. Magari M, et al. 2009. Enhancement of antibody production from a chicken B cell line DT40 by reducing Pax5 expression. *J. Biosci. Bioeng.* 107:206–209.
19. Kajita M, et al. 2010. Efficient affinity maturation of antibodies in an engineered chicken B cell line DT40-SW by increasing point mutation. *J. Biosci. Bioeng.* 110:351–358.
20. Bachl J, Ertongur I, Jungnickel B. 2006. Involvement of Rad18 in somatic hypermutation. *Proc. Natl. Acad. Sci. U. S. A.* 103:12081–12086.
21. Arakawa H, et al. 2006. A role for PCNA ubiquitination in immunoglobulin hypermutation. *PLoS Biol.* 4:e366.
22. Aoufouchi S, et al. 2008. Proteasomal degradation restricts the nuclear lifespan of AID. *J. Exp. Med.* 205:1357–1368.
23. Feng YQ, et al. 1999. Site-specific chromosomal integration in mammalian cells: highly efficient CRE recombinase-mediated cassette exchange. *J. Mol. Biol.* 292:779–785.
24. Toledo F, Liu CW, Lee CJ, Wahl GM. 2006. RMCE-ASAP: a gene targeting method for ES and somatic cells to accelerate phenotype analyses. *Nucleic Acids Res.* 34:e92.
25. Wong ET, et al. 2005. Reproducible doxycycline-inducible transgene expression at specific loci generated by Cre-recombinase mediated cassette exchange. *Nucleic Acids Res.* 33:e147.
26. Han L, Masani S, Yu K. 2011. Overlapping activation-induced cytidine deaminase hotspot motifs in Ig class-switch recombination. *Proc. Natl. Acad. Sci. U. S. A.* 108:11584–11589.
27. Sale JE, et al. 2001. *In vivo* and *in vitro* studies of immunoglobulin gene somatic hypermutation. *Philos. Trans. R. Soc. Lond. B Biol. Sci.* 356: 21–28.
28. Harris RS, Croom-Carter DS, Rickinson AB, Neuberger MS. 2001. Epstein-Barr virus and the somatic hypermutation of immunoglobulin genes in Burkitt's lymphoma cells. *J. Virol.* 75:10488–10492.
29. Martin A, et al. 2002. Activation-induced cytidine deaminase turns on somatic hypermutation in hybridomas. *Nature* 415:802–806.
30. Zhang W, et al. 2001. Clonal instability of V region hypermutation in the Ramos Burkitt's lymphoma cell line. *Int. Immunol.* 13:1175–1184.
31. Cumbers SJ, et al. 2002. Generation and iterative affinity maturation of antibodies *in vitro* using hypermutating B-cell lines. *Nat. Biotechnol.* 20: 1129–1134.
32. Green NS, Lin MM, Scharff MD. 1998. Ig hypermutation in cultured cells. *Immunol. Rev.* 162:77–87.
33. Martin A, Scharff MD. 2002. Somatic hypermutation of the AID transgene in B and non-B cells. *Proc. Natl. Acad. Sci. U. S. A.* 99:12304–12308.
34. Yang SY, Schatz DG. 2007. Targeting of AID-mediated sequence diversification by *cis*-acting determinants. *Adv. Immunol.* 94:109–125.
35. Maquat LE. 2004. Nonsense-mediated mRNA decay: splicing, translation and mRNP dynamics. *Nat. Rev. Mol. Cell Biol.* 5:89–99.
36. Woo CJ, Martin A, Scharff MD. 2003. Induction of somatic hypermutation is associated with modifications in immunoglobulin variable region chromatin. *Immunity* 19:479–489.
37. Sale JE, Neuberger MS. 1998. TdT-accessible breaks are scattered over the immunoglobulin V domain in a constitutively hypermutating B cell line. *Immunity* 9:859–869.
38. Di Noia JM, Neuberger MS. 2007. Molecular mechanisms of antibody somatic hypermutation. *Annu. Rev. Biochem.* 76:1–22.
39. Zarrin AA, et al. 2004. An evolutionarily conserved target motif for immunoglobulin class-switch recombination. *Nat. Immunol.* 5:1275–1281.
40. Beale RC, et al. 2004. Comparison of the differential context-dependence of DNA deamination by APOBEC enzymes: correlation with mutation spectra *in vivo*. *J. Mol. Biol.* 337:585–596.
41. Martomo SA, Yang WW, Gearhart PJ. 2004. A role for Msh6 but not Msh3 in somatic hypermutation and class switch recombination. *J. Exp. Med.* 200:61–68.
42. Martomo SA, et al. 2005. Different mutation signatures in DNA polymerase  $\epsilon$ - and MSH6-deficient mice suggest separate roles in antibody diversification. *Proc. Natl. Acad. Sci. U. S. A.* 102:8656–8661.
43. Min IM, Rothlein LR, Schrader CE, Stavnezer J, Selsing E. 2005. Shifts in targeting of class switch recombination sites in mice that lack mu switch region tandem repeats or Msh2. *J. Exp. Med.* 201:1885–1890.
44. Manis JP, Tian M, Alt FW. 2002. Mechanism and control of class-switch recombination. *Trends Immunol.* 23:31–39.
45. Wang L, Jackson WC, Steinbach PA, Tsien RY. 2004. Evolution of new nonantibody proteins via iterative somatic hypermutation. *Proc. Natl. Acad. Sci. U. S. A.* 101:16745–16749.
46. Basu U, et al. 2005. The AID antibody diversification enzyme is regulated by protein kinase A phosphorylation. *Nature* 438:508–511.
47. Cheng HL, et al. 2009. Integrity of the AID serine-38 phosphorylation site is critical for class switch recombination and somatic hypermutation in mice. *Proc. Natl. Acad. Sci. U. S. A.* 106:2717–2722.
48. Yamane A, et al. 2011. Deep-sequencing identification of the genomic targets of the cytidine deaminase AID and its cofactor RPA in B lymphocytes. *Nat. Immunol.* 12:62–69.
49. Chaudhuri J, Khuong C, Alt FW. 2004. Replication protein A interacts with AID to promote deamination of somatic hypermutation targets. *Nature* 430:992–998.
50. Bransteitter R, Pham P, Calabrese P, Goodman MF. 2004. Biochemical analysis of hypermutational targeting by wild type and mutant activation-induced cytidine deaminase. *J. Biol. Chem.* 279:51612–51621.
51. Michael N, et al. 2003. The E box motif CAGGTG enhances somatic hypermutation without enhancing transcription. *Immunity* 19:235–242.
52. Carpenter MA, Rajagurubandara E, Wijesinghe P, Bhagwat AS. 2010. Determinants of sequence-specificity within human AID and APOBEC3G. *DNA Repair (Amst.)* 9:579–587.
53. Kohli RM, et al. 2009. A portable hot spot recognition loop transfers sequence preferences from APOBEC family members to activation-induced cytidine deaminase. *J. Biol. Chem.* 284:22898–22904.
54. Wang M, Rada C, Neuberger MS. 2010. Altering the spectrum of immunoglobulin V gene somatic hypermutation by modifying the active site of AID. *J. Exp. Med.* 207:141–153.
55. Wang M, Yang Z, Rada C, Neuberger MS. 2009. AID upmutants isolated using a high-throughput screen highlight the immunity/cancer balance limiting DNA deaminase activity. *Nat. Struct. Mol. Biol.* 16:769–776.
56. Milstein C, Neuberger MS, Staden R. 1998. Both DNA strands of antibody genes are hypermutation targets. *Proc. Natl. Acad. Sci. U. S. A.* 95: 8791–8794.
57. Frey S, et al. 1998. Mismatch repair deficiency interferes with the accumulation of mutations in chronically stimulated B cells and not with the hypermutation process. *Immunity* 9:127–134.
58. Rada C, Ehrenstein MR, Neuberger MS, Milstein C. 1998. Hot spot focusing of somatic hypermutation in MSH2-deficient mice suggests two stages of mutational targeting. *Immunity* 9:135–141.



59. Wagner SD, Elvin JG, Norris P, McGregor JM, Neuberger MS. 1996. Somatic hypermutation of Ig genes in patients with xeroderma pigmentosum (XP-D). *Int. Immunol.* **8**:701–705.
60. Larijani M, et al. 2007. AID associates with single-stranded DNA with high affinity and a long complex half-life in a sequence-independent manner. *Mol. Cell. Biol.* **27**:20–30.
61. Pham P, Calabrese P, Park SJ, Goodman MF. 2011. Analysis of a single-stranded DNA-scanning process in which activation-induced deoxycytidine deaminase (AID) deaminates C to U haphazardly and inefficiently to ensure mutational diversity. *J. Biol. Chem.* **286**:24931–24942.
62. Ta VT, et al. 2003. AID mutant analyses indicate requirement for class-switch-specific cofactors. *Nat. Immunol.* **4**:843–848.
63. Dickerson SK, Market E, Besmer E, Papavasiliou FN. 2003. AID mediates hypermutation by deaminating single stranded DNA. *J. Exp. Med.* **197**:1291–1296.
64. Chelico L, Pham P, Petruska J, Goodman MF. 2009. Biochemical basis of immunological and retroviral responses to DNA-targeted cytosine deamination by activation-induced cytidine deaminase and APOBEC3G. *J. Biol. Chem.* **284**:27761–27765.
65. Ford GS, Yin CH, Barnhart B, Sztam K, Covey LR. 1998. CD40 ligand exerts differential effects on the expression of I gamma transcripts in subclones of an IgM+ human B cell lymphoma line. *J. Immunol.* **160**:595–605.
66. Bookout AL, Cummins CL, Mangelsdorf DJ, Pesola JM, Kramer MF. 2006. High-throughput real-time quantitative reverse transcription PCR. *Curr. Protoc. Mol. Biol.* Chapter 15:Unit 15.8.